3D Image Correlation Studies of Geometry and Material Property Effects During Split Hopkinson Bar Experiments

Tim Schmidt, Trilion Quality Systems, 200 Barr Harbor Dr. Suite 400, West Conshohocken, PA 19428
Amos Gilat, Andrew Walker and Jeremy Seidt, The Ohio State University, Columbus, Ohio, 43210
John Tyson, Trilion Quality Systems

ABSTRACT

Full field measurement of strain and strain rate in split Hopkinson bar experiments using the Aramis three-dimensional image correlation system has previously been thoroughly validated. Local strains and 3D displacements are measured at thousands of points, with data acquisition rates as high as 300,000 frames per second. The new capability of direct full-field local strain measurements at high strain rates provides orders of magnitude more information than the traditional method of inferring the average specimen strain based on elastic wave behavior. For example, now the dynamic necking behavior of a ductile specimen can be directly observed, and valid strains can be obtained regardless of whether stress equilibrium and strain homogeneity exist. Shear bands and complex local strain fields can be quantified.

Aramis strains for OFHC copper and 2024 aluminum are compared to a specimen gauge and to elastic wave results. In compression and shear, the results agree, but it is found that in tension, there can be errors in the elastic wave results due to significant deformation outside the gauge region. The influence of specimen geometry and material properties on the accuracy of the elastic wave strain time history and stress/strain curves is explored. The ability to profile a shear localization throughout the complete load time history for a torsion test is also presented.

INTRODUCTION

The Split-Hopkinson Bar (SHB) technique (also called the Kolsky bar) is the most commonly used method of measuring material behavior (stress-strain curve) at strain rates between about 400 s^{-1} and 5,000 s^{-1}. A small material specimen is placed between two bars. The specimen is loaded by a stress wave that is generated in one of the bars (incident). As the specimen is loaded, part of the wave propagates through to the other bar (transmitter), and part is reflected back to the incident bar. The dimensions of the bars and the specimen, and the amplitude of the loading wave are designed such that during the test, the specimen is loaded beyond the elastic limit, while the bars remain elastic. Using elastic wave theory, the force, strain rate and strain in the specimen can be determined from the stress waves in the bars. The technique was introduced with compression loading by Kolsky [1], and has subsequently been modified for tension and torsion applications.

In a typical compression SHB experiment [2] the specimen (a short small diameter cylinder) is placed between the incident and transmitter bars. A lubricant is applied at the contact surfaces, and it is assumed that the specimen is loaded only by an axial compression force, since the lubricant prevents any shear traction on the end surfaces as the specimen is deformed. It is also assumed that the deformation is uniform, such that the whole specimen is under a uniform state of uniaxial compression throughout the test. With these assumptions, the stress in the specimen is calculated by dividing the force in the specimen (determined from the transmitted wave) by the cross-sectional area. The strain rate is the difference between the velocities of the end surfaces of the specimen (given by the wave that is reflected back from the specimen to the incident bar) divided by its length. The strain is determined by integrating the strain rate. Experiments show that up to about 30% axial strain, the specimen remains cylindrical in shape, but at larger strains the specimens start to barrel, which obviously means that the specimen at that stage is no longer under a uniform state of uniaxial compression.

Tensile SHB tests are more difficult to conduct and analyze. A typical specimen for a tensile test has a dogbone geometry, with a middle section of small cross-sectional area (gage section) and ends with a larger cross-sectional area. Rounded fillets comprise the transition from the gage section to the larger ends, which are attached to the bars of the SHB apparatus. The specimen has to be designed such that most of the gage section is under a state of uniaxial tension. As in the compression test, the stress is calculated by dividing the force in the specimen (determined from the transmitted wave) by the cross-sectional area. The determination of the strain rate in a tensile SHB test is more involved, because the portion of the specimen coupon between the ends of the bars includes both the central gage section and the rounded fillets. If the deformation is confined only to the gage section, then the strain rate can accurately be calculated by dividing the difference between the velocities of the end of the bars by the length of the gage section. In reality, however, at least some of the relative motion between the bars is due to deformation within the fillets. How much deformation is actually taking place in the fillet depends on the dimensions and the material properties of the specimen. This aspect of the tensile SHB experiment is carefully examined in the present paper.

3D image correlation photogrammetry is a full-field displacement and strain measurement tool increasingly used for static and slow rate testing [3-5], which has also been applied for numerous dynamic applications using digital high speed cameras [6-7]. The object being tested is viewed by a stereo pair of high-resolution digital cameras. Sample preparation consists of applying a regular or random high contrast dot pattern to the surface, commonly with spray paint, which will deform with the substrate. Thousands of overlapping unique correlation areas known as facets (typically 15 pixels square) are defined across the entire imaging area. The center of each facet is a measurement point that can be thought of as a 3D displacement sensor. Pairs of them become extensometers, and arrays of these closely spaced gauges form in-plane strain rosettes. The facet centers are tracked, in each successive pair of images, with accuracy up to 0.003 pixel. Then, using the principles of photogrammetry, the 3D coordinates of each facet are determined for each picture set. The results are the 3D shape of the component, the 3D displacements, and the in-plane strains. Data can be presented as color plots, movies, section line diagrams, etc, and ASCII exports support further analysis and comparison. Because of similar output, 3D image correlation is an excellent tool for verifying and iterating finite element models; it provides distribution as well as maximum values of displacements and strains. The method is extremely robust. It has wide dynamic range and is not affected by rigid body motions, ambient vibrations, etc. The key feature that is exploited when using high speed cameras is that simply put, as long as pairs of non-blurred pictures can be captured, 3D coordinates, 3D displacements and the in-plane strains can be measured. The basic principles of 3D image correlation photogrammetry have been known for about 15 years [4]. The particular 3D image correlation system used for this investigation, ARAMIS, has been commercially available for more than 10 years, and has an installed base of about 350 systems worldwide. Tests were conducted with Photron APX RS cameras on specimens made of as-received and annealed copper. The effect of the specimen geometry in tensile tests is investigated by testing specimens with different gage lengths.

PRIOR VALIDATION OF 3D IMAGE CORRELATION FOR HOPKINSON BAR TESTS

During the past two years, the authors have extensively validated Aramis 3D image correlation results through detailed comparison to elastic waves and specimen strain gauges [8-9]. Initially, well-characterized tension specimens that were known to have homogeneous strain and achieve stress equilibrium were used. Later, extensive repeatability studies on compression specimens were conducted. A typical benchmark result comparing the image correlation and elastic wave based strain time histories is shown in Figure 1; note the excellent agreement. A comparison for an as-received tension specimen in which necking occurred is shown in Figure 2. There is early agreement until necking occurs, when the average strain from the elastic waves is lower than the local result in the necking region.

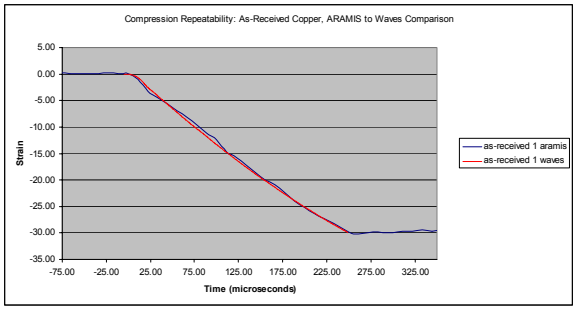

Figure 1: Comparison of image correlation and elastic wave based strain time histories for an as-received copper compression specimen.

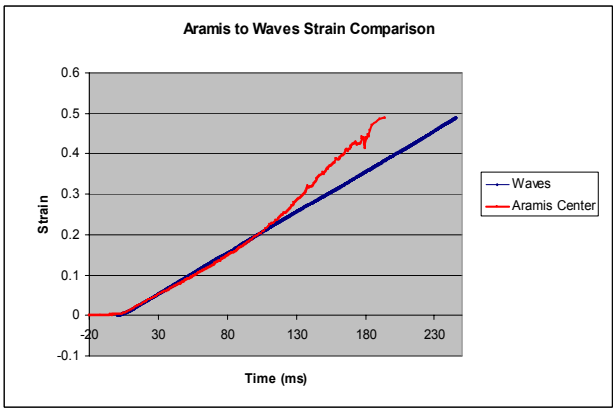

Figure 2: Comparison of image correlation and elastic wave based strain time histories for an as-received copper tension specimen in which necking occurred.

COMPRESSION SPLIT HOPKINSON BAR TESTS

The compression SHB apparatus used for the tests is made of 12.7 mm diameter Ti-6Al-4V bars. The projectile generating the loading wave has a length of 609.6 mm. The specimens made of 101000 copper are circular cylinders with a diameter of 5.08 mm and length of 6.35 mm machined from a bar. Tests are done with as-received and annealed (350^{o}C for one hour and furnace cooled) material. A strain gage is placed directly on the specimen. The contact faces between the specimen and the bars are lubricated with Molybdenum Disulfide grease to limit friction during the test. A high contrast pattern is applied on one side of the specimen with spray paint using a dot-on-dot method. This method consists of first spraying a fine mist of white paint onto the specimen, leaving a pattern of white dots with some bare copper showing through, and then spraying a fine mist of black paint to cover the bare copper. The painted specimen positioned between the bars is shown in Figure 3. The frame rate of the Photron cameras is 105,000 frames per second (approximately 9.5 microseconds between frames), with a resolution of 128 by 80 pixels. The determination of the strain with Aramis is done by using overlapping virtual strain gages that are approximately 1.1 mm long.

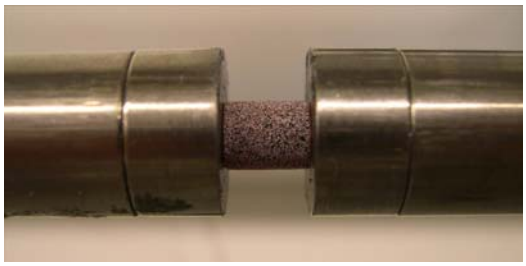

Figure 3: A patterned copper specimen in the compression SHB apparatus.

Results from a typical test with a specimen made of as-received copper are shown in Figures 4-6 (in Figures 4 and 5, compression values are shown as positive). The waves recorded on the incident and transmitter bars and the strain measured by the strain gage that is placed directly on the specimen are displayed in Figure 4. The time histories for stress (engineering), strain rate and strain (determined from the waves in the bars), strain measured by the strain gage on the specimen, and strain measured with the Aramis system at a point in the middle of the specimen are shown in Figure 5. This figure shows that the strains measured with the different techniques agree well with each other. The strain rate as determined by the SHB analysis from the reflected wave is about 1100 s^{-1} in the beginning and decreases during the test to 800 s^{-1} (average taken as 950 s^{-1}). The axial strain measured with the image correlation method along the specimen is shown in Figure 6. The figure shows the strain every third frame, or approximately every 28.5 microseconds. Overall, the strain along the specimen is uniform. There is a slight reduction in the strain near the right end (possibly due to some friction on that face), and there is some non-uniform deformation at the left side of the specimen as the strain approaches 20%.

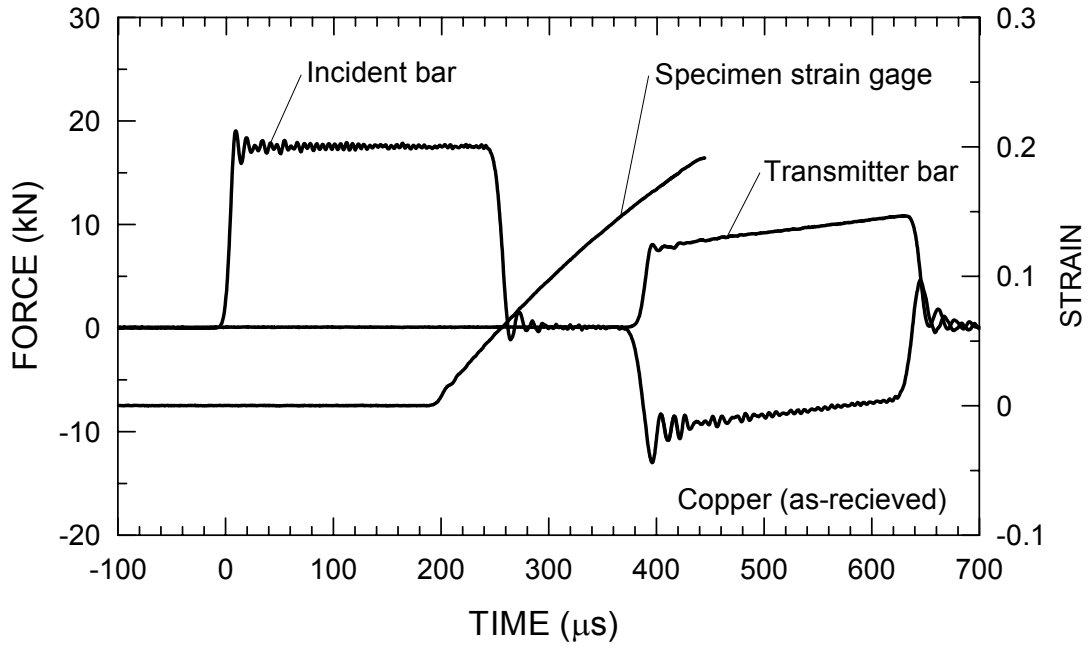

Figure 4: Data recorded in a compression SHB test (copper, as-received).

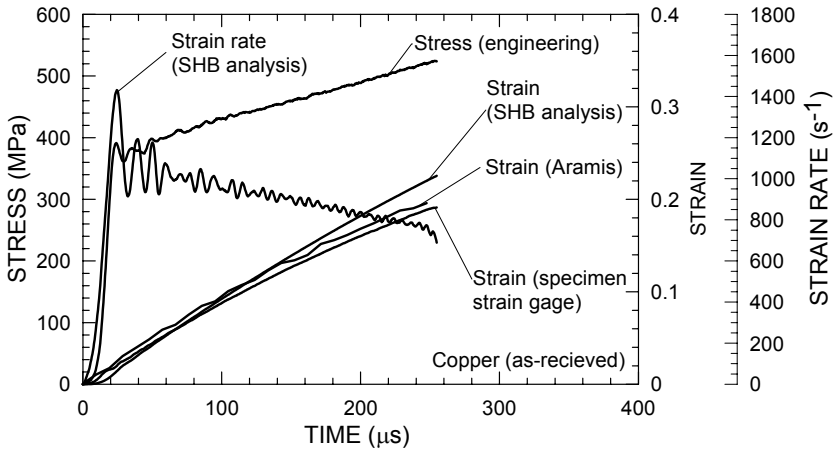

Figure 5: Stress, strain rate and strain in a compression SHB test (copper, as-received).

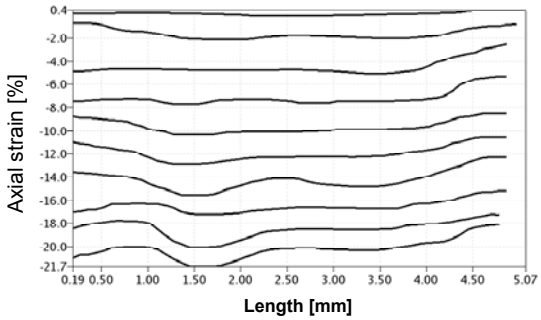

Figure 6: Aramis section line results showing generally uniform strain distribution along the specimen in a compression SHB test (copper, as-received).

TENSILE SPLIT HOPKINSON BAR TESTS

The tensile SHB apparatus, Staab and Gilat [10], shown schematically in Figure 7, is made of 12.7 mm diameter 7075 aluminum bars. The loading tensile wave in the incident bar is generated by the release of a tensile load that is initially stored at the end section of the bar. The elastic waves are measured at two locations on the incident bar and in one location on the transmitter bar (Gages A, B and C in Figure 7). The flat dog-bone shaped specimens, Figure 8, are machined from a plate. The specimens are attached to the bars by cementing the end tabs into notched aluminum adaptors, which are then glued to the ends of the split Hopkinson bars, Figure 8b. A high contrast black and white dot pattern is applied to one face of the specimen, and a strain gage is placed on the back face of the specimen. During a test, the region between the ends of the incident and transmitter bars includes the gage section (the middle part of the specimen where the sides are parallel) and the adjacent rounded fillets in the transition between wide end tabs and the narrower gage section. The state of stress and deformation in the gage section and the adjacent rounded fillets during a test depends on the dimensions and the material properties (yield stress and hardening rate) of the specimen material. In an ideal test, plastic deformation in confined to the gage section, which is under uniform uniaxial tension and the stresses in the fillets are below the elastic limit. In this case, the strain rate, strain, and stress that are determined from the recorded waves give an accurate measure of the material response. In a real test, however, it is unlikely that no plastic deformation takes place outside the gage section. Examination of the effect of the specimen's mechanical properties on the accuracy of the measurements is done by conducting tests with specimens made of as-received and annealed (350^{o}C for one hour and furnace cooled) 101000 copper. The effect of the specimen's geometry is investigated by using specimens with gage lengths of 6.4 and 2.54 mm. The frame rate of the Photron cameras is 112,500 frames/s (approximately 8.9 microseconds between frames), with a resolution of 256 by 48 pixels. The determination of the strain with Aramis is done by using overlapping virtual gages that are approximately 2.4 mm long.

Results from a test with a specimen made of as-received copper, with a gage length of 6.35 mm, are shown in Figures 9-12. The average strain rate, strain, and stress in the specimen versus time that are determined from the recorded waves in the bars (SHB analysis) are shown in Figure 9. This figure shows also the strain measured directly on the specimen with the strain gage, and the strain measured at the center of the specimen with the Aramis system. It can be seen that up to the point when the necking starts (at about 400 μs), all of the strain measurements agree well with each other. When the localization (necking)

starts, the Aramis shows a sharp increase in the strain, similar to what was seen in Figure 2. The strain rate as determined from the SHB analysis is about 600 s^{-1}. The axial strain measured with the image correlation method along the specimen is shown in Figure 10. The figure shows the strain for every fifth frame, or approximately every 44.5 μs. This waterfall plot shows that in the early part of the test, the strain is nearly uniform along 70% of the gage length. As the specimen deforms, the length of the portion of the gage section that is under uniform deformation decreases gradually until the necking develops. The strain near the ends of the gage section is smaller. Figure 10 shows also that only a very small amount of plastic deformation is taking place outside the gage section in the rounded fillets. This is further confirmed by the full-field plot of Figure 11. It is important to note that, as shown in Figure 9, the strain measured with Aramis at the center of the specimen is essentially the same (before the necking) as the average strain determined from the elastic waves in the bars. The latter is calculated by dividing the relative displacement between the incident and transmitter bar by the length of the gage section. The relative displacement includes displacement due to the deformation outside the gage section in the rounded fillets. This "extra" displacement compensates for the smaller deformation in the gage section near its ends, and the overall average strain calculated with the SHB analysis ends up to be the same as measured with the Aramis system at the center of the specimen. Two (engineering) stress strain curves from this test, that are nearly identical, are shown in Figure 12. One curve uses the strain from the SHB analysis and the other uses the strain from Aramis.

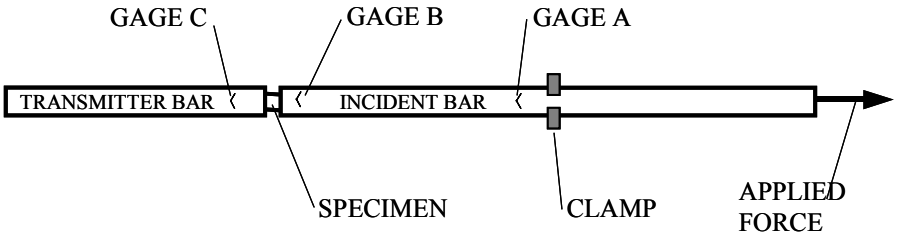

Figure 7: Schematic of the tensile split Hopkinson bar apparatus.

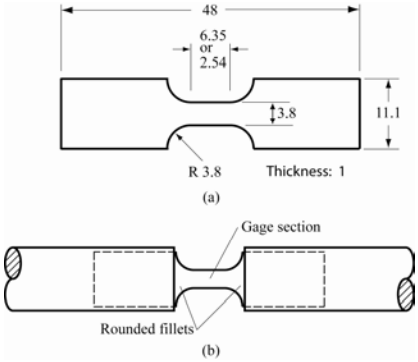

Figure 8: (a) Tensile specimen. (b) Tensile specimen in the SHB apparatus.

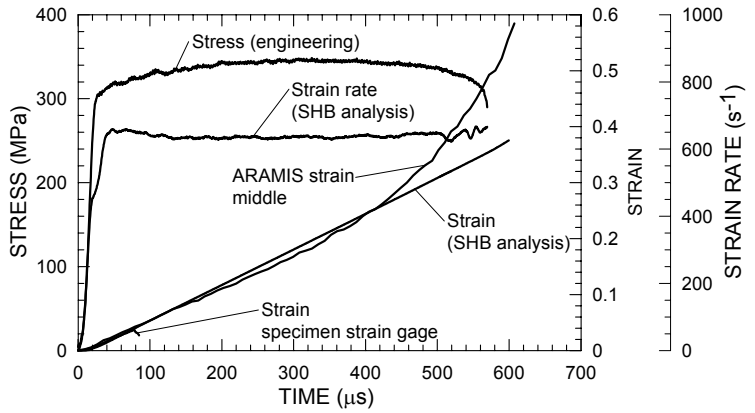

Figure 9: Stress, strain rate, and strain in test with as received copper (gage length 6.35 mm).

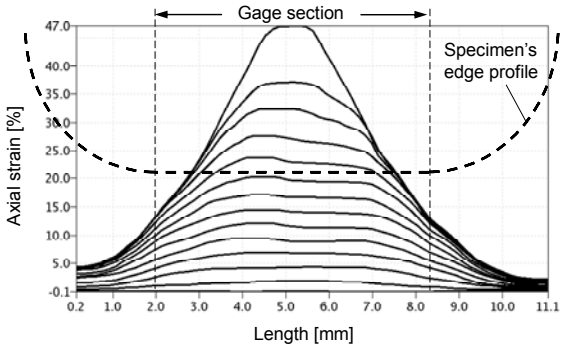

Figure 10: Strain distribution along the specimen (as received copper, gage length 6.35 mm). The progression of necking over time is clearly indicated.

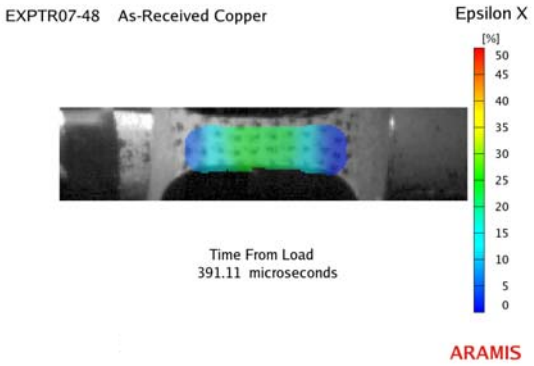

Figure 11: Strain map overlay on camera image for as-received copper. Note that the strain outside the gage region is extremely low.

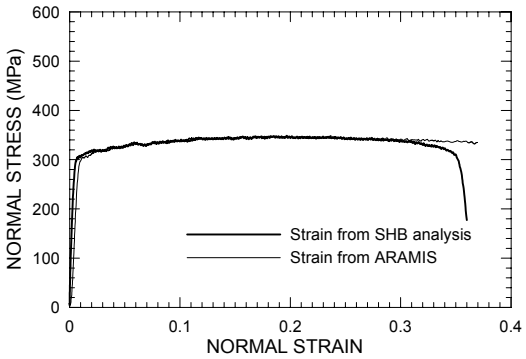

Figure 12: Tension stress-strain curves of as-received copper (gage length 6.35 mm).

Results from a test with a specimen made of as received copper with a gage length of 2.54 mm are shown in Figures 13 through 15. The average strain rate, strain, and stress in the specimen versus time that are determined from the recorded waves in the bars (SHB analysis) are shown in Figure 13, which also includes the strain measured directly on the specimen with the strain gage, and the strain measured at the center of the specimen with the Aramis system. Here we can see a noticeable difference between the strain determined from the waves and the strain measured with Aramis in the center. The strain measured by the strain gage that is on the specimen agrees with the strain measured with Aramis. The strain rate according to the SHB analysis is approximately 1600 s^{-1},while an estimation of the average strain rate from the slope of the strain versus time plot of the strain measured with Aramis gives 1250 s^{-1}. The distribution of the strain along the specimen as measured with the image correlation method is shown in Figure 14. The figure shows the strain every fifth frame, or approximately every 44.5 μs. This waterfall plot shows that less than half of the gage length is under uniform strain. There is

also a significant plastic deformation outside the gage section in the rounded fillets, which in this specimen have a length similar to the gage section. The average strain determined from the waves, which assumes that all of the deformation between the bars (including in the fillets) is due to deformation in the gage length, is significantly larger than the strain measured by Aramis at the center of the gage length. Two (engineering) stress strain curves from this test (one with strain measured with Aramis and one with strain determined from the waves) are shown in Figure 15. Since the as-received copper does not have much hardening, the two stress strain curves appear close to each other up to a strain of 0.25. At this point, the curve that uses the strain from Aramis shows necking, while the curve that uses the SHB strain continues to a strain of at least 0.35 before the necking starts.

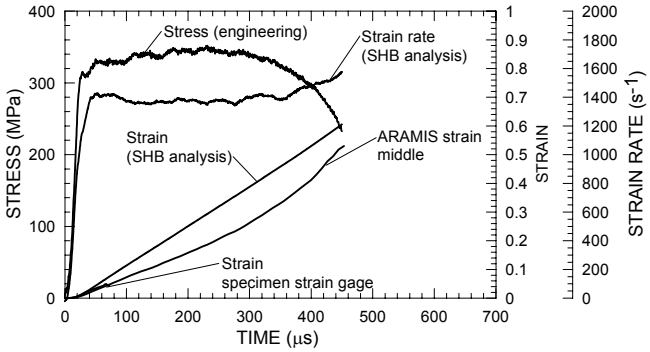

Figure 13: Stress, strain rate, and strain in test with as received copper (gage length 2.54 mm).

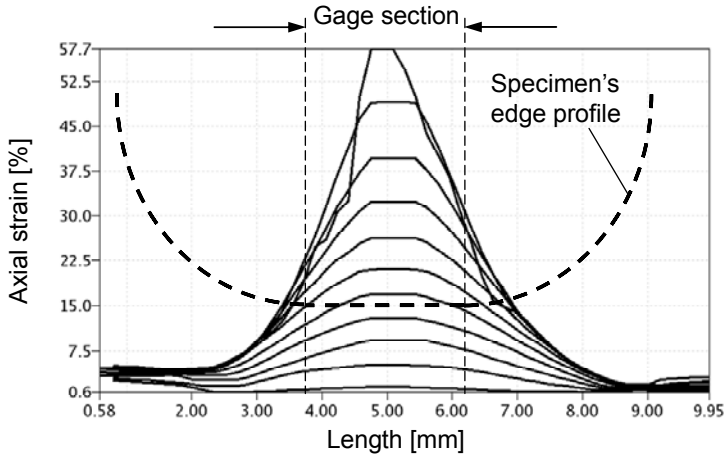

Figure 14: Strain distribution along the specimen (as received copper, gage length 2.54 mm).

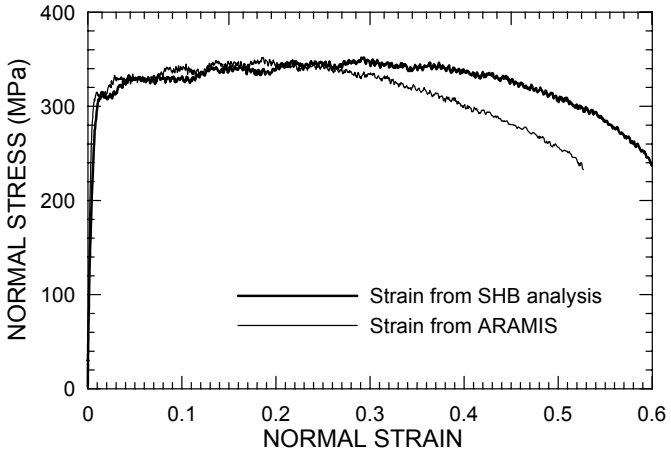

Figure 15: Tension stress-strain curves of as received copper (gage length 2.54 mm).

Results from a test with a specimen made of annealed copper with a gage length of 6.35 mm are shown in Figures 16 through 18. The average strain rate, strain, and stress in the specimen versus time that are determined from the recorded waves in the bars (SHB analysis) are shown in Figure 16. This figure also shows the strain measured directly on the specimen with the strain gage, and the strain measured at the center of the specimen with the Aramis system. Here there is a large difference between the strain determined from the waves and the strain measured with Aramis. The strain measured by the strain gage that is on the specimen agrees with the strain measured with Aramis. The strain rate according to the SHB analysis ranges from about 1000 s^{-1} at the beginning of the stress to about 800 s^{-1} at the end of the test. An estimation of the average strain rate from the slope of the strain versus time plot of the strain measured with Aramis gives a much smaller value of 430 s^{-1}. The distribution of the strain along the specimen as measured with the image correlation method is shown in Figure 17. This waterfall plot shows that most of the gage section is under uniform strain and that a significant amount of plastic deformation is taking place in the rounded fillets outside the gage section. This is happening because the yield stress of the annealed copper is very small (about 30 MPa) and strain hardening due to plastic deformation is very large. As the material in the gage section deforms and hardens, the applied force increases. The stress in the rounded fillets and the tabs is smaller than in the gage section since the cross-sectional area is larger, but this does not prevent plastic deformation since the yield stress is small. Examination of the specimen after the test shows that even the tabs inside the aluminum adaptors undergo noticeable plastic deformation. All of this deformation that actually occurs outside the gage section is assumed to occur in the gage section when the average strain is determined from the waves in the bars. Two (engineering) stress strain curves from this test (one with strain measured with Aramis and one with strain determined from the waves) are shown in Figure 18. The correct material response is represented by the curve that uses the Aramis strain, and is significantly steeper than the curve that uses the strain determined from the waves in the bars.

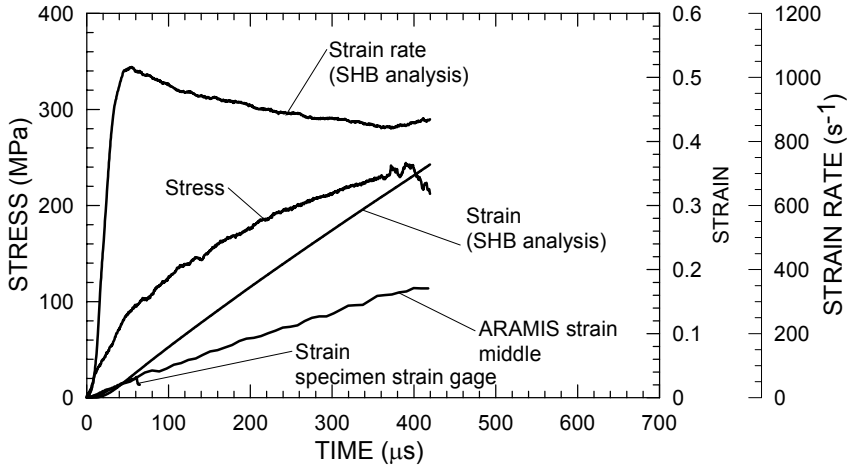

Figure 16: Stress, strain rate, and strain in test with as annealed copper (gage length 6.35 mm).

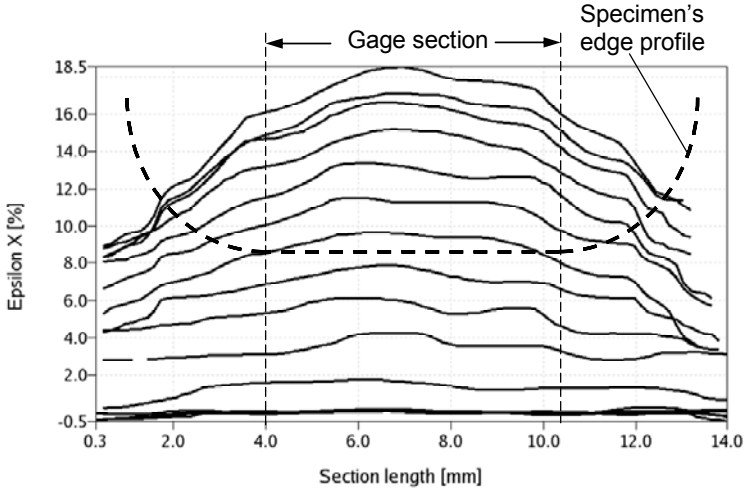

Figure 17: Strain distribution along the specimen (annealed copper, gage length 6.35 mm). Note that significant deformation is occurring outside the gage region.

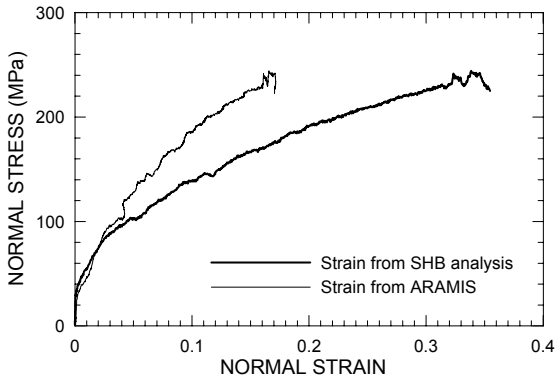

Figure 18: Stress-strain curves, annealed copper (gage length 6.35 mm). Note that the Aramis data comprises a much steeper curve than the elastic wave results.

TORSION TESTING

Torsion testing was conducted on a copper specimen with a small circumferential notch on the inside diameter. The machinist estimated that the notch width was 0.015", and the depth was 0.010". A shear localization occurred, and this was measured through the complete load.

Uniformity of the strain field outside of the localization was excellent, as seen in Figure 19. Note that the entire load history is captured, as indicated by the plateau in peak strain after approximately 850 microseconds. Significant "orange peel" surface deformations were evident post-test, as shown in the micrograph of Figure 20. Figure 21 shows the evolution of the shear localization with load increase. Sufficient data remains present despite the rotation of the specimen, and the paint pattern did not detach or deteriorate. The strain profile across the gage length, indicating the width and peak strain of the shear localization, is shown in Figure 22. The waterfall plot of Figure 23 shows the increasing magnitude of strain across a constant width.

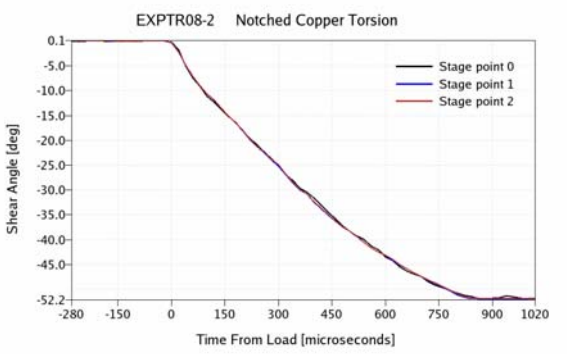

Figure 19: Strain uniformity at various points outside the notched region on a torsion specimen is excellent. The entire load history has been captured, as indicated by the plateau in peak strain after approximately 850 microseconds.

Figure 20: Post-test photo showing "orange peel" surface deformations in the notched region (non-painted area).

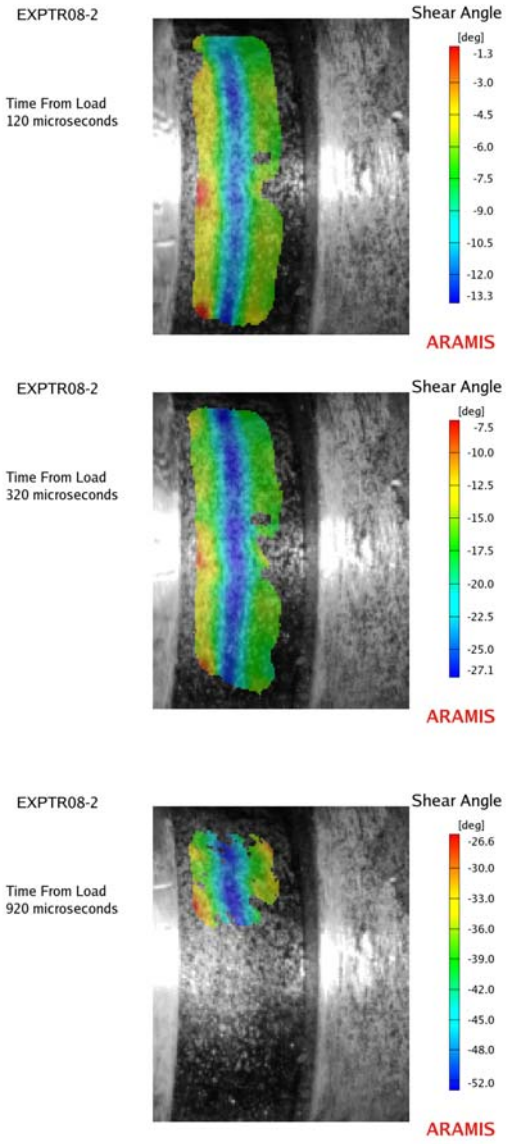

Figure 21: Full-field results showing the evolution of strain in a notched torsion specimen.

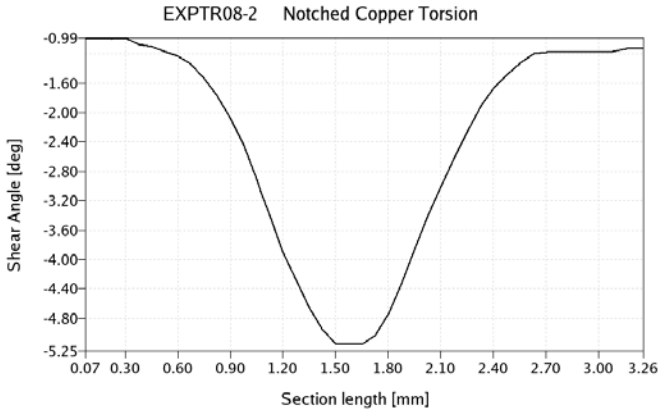

Figure 22: Section line profile indicating width and peak strain in notch region.

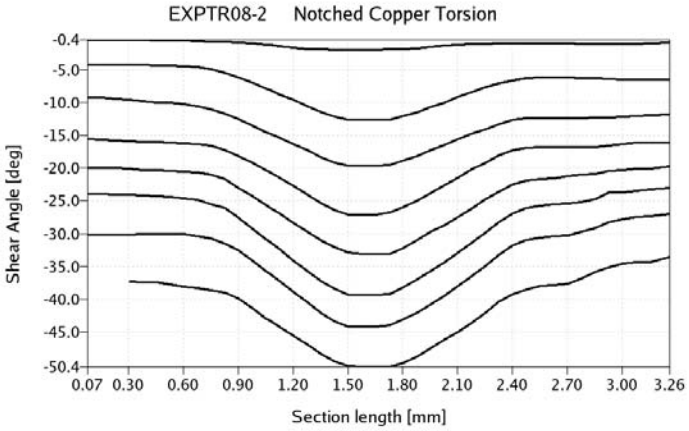

Figure 23: Waterfall plot showing evolution of strain across gage region with notch.

CONCLUSIONS

The 3D image correlation technique for full field measurement of strains on the surface of a specimen can be used in experiments involving high rates of deformation. Results from compression SHB tests with specimens made of as-received and annealed copper shows that the deformation of the specimen is uniform. In this case, the strain measured using image correlation is in agreement with the strain measured with a strain gage directly on the specimen and also with the strain that is determined in the traditional SHB technique from the reflected wave in the incident bar.

In tensile SHB experiments, image correlation gives the full field distribution of the strain throughout the test, including during the necking. When applicable (the first few percent of deformation), the axial strain measured with image correlation agrees well with the strain measured with a strain gage that is attached to the specimen. The average strain that is determined from the elastic waves in the bars is not always the same as the strain that is measured with image correlation at the center of the specimen's gage section. The strain distribution within the gage section and in the rounded fillets adjacent to the gage section depends on the exact geometry and properties (yield stress and strain hardening rate) of the specimen. If most of the gage section is under a uniform uniaxial state of stress, and if the deformation outside the gage section is relatively small, then the average strain that is determined from the waves in the bars is comparable with the strain that is measured with image correlation in the center of the gage section. If only a small portion of the gage section is under a uniform uniaxial state of stress, and if the deformation outside the gage section is relatively large, then the average strain that is determined from the waves in the bars can differ significantly from the strain that is measured with image correlation in the center of the gage section.

Tests with dogbone shaped specimens made of as-received copper with gage lengths of 6.35 mm show that before necking, most of the gage section is under a state of uniform tensile strain. Near the ends of the gage section, the strains are smaller and some plastic deformation is taking place outside the gage section. The average strain that is determined from the elastic waves in the bars agrees with the strain measured with image correlation at the center of the specimen. In tests with a specimen with a shorter gage length of 2.54 mm, less than half of the gage length is under a state of uniform uni-axial tension, and some plastic deformation is taking place outside the gage section. In these tests, the average strain that is determined from the elastic waves in the bars is larger than the strain measured with image correlation at the center of the specimen. In tests with specimens made of annealed copper and a gage length of 6.35 mm, the strain determined from the elastic waves in the bars is significantly larger than the strain measured with image correlation at the center of the specimen. The difference is due to large plastic deformation outside the gage section, because the annealed copper has a very low yield stress and a very high strain hardening rate.

The ability to quantify shear localizations during torsion testing was demonstrated. Significant orange peel surface deformations and rotation of the specimen during the test do not prevent data acquisition.

3D image correlation using digital high-speed cameras has been shown to provide significant benefits for the accurate determination of local strains during compression, tension and torsion split Hopkinson Bar testing. Direct measurement of thousands of local strains is superior to inference of average strain based on assumptions of equilibrium and uniformity which do not always occur in practice.

ACKNOWLEDGEMENTS

The research reported in this paper was supported by the Air Force SBIR Phase I Contract FA8651-05-C-0223 and Phase II Contract FA8651-06-C-0123, "Revolutionary Materials Research Technology For High-Strain Rate Ordnance Research". The technical sponsor is Dr. Joel House and the technical monitor is Mr. Philip Flater.

Thanks to Gary Gardner for specimen and adaptor machining.

REFERENCES

1. Kolsky, H., "An Investigation of the Mechanical Properties of Materials at Very High Rates of Loading," Proc. Phys. Soc., London, **62-B**, 676-700 (1949).

2. Gray, G.T., "Classic Split-Hopkinson Pressure Bar Testing," ASM Handbook, Vol. 8, Mechanical Testing and Evaluation, ASM International, Materials Park, Ohio, 462-476 (2000).

3. Kahn-Jetter, Z.L. and Chu, T.C., "3-D Displacement Measurements Using Digital Image Correlation and Photogrammetry Techniques," Exp. Mech., **30 (1)**, 10-16 (1990).

4. Helm, J.D., McNeill, S.R., and Sutton, M.A., Z.L., "Improved Three-Dimensional Image Correlation for Surface Displacement Measurement," Opt. Eng., **35 (7)**, 1911-1920 (1996).

5. Schmidt, Tyson and Galanulis, Full-Field Dynamic Displacement and Strain Measurement Using Advanced 3D Image Correlation Photogrammetry, Experimental Techniques, Part I: May/June 2003, Vol. 27 #3, p.47-50, Part II: July/Aug, Vol. 27 #4, p.44-47.

6. Schmidt, Tyson, Revilock et al, Performance Verification of 3D Image Correlation Using Digital High-Speed Cameras, Proceedings of the SEM Annual Conference and Exposition, Portland, OR, June 7-9, 2005.

7. Schmidt, Tyson, Galanulis, Revilock and Melis, Full-field dynamic deformation and strain measurements using high-speed digital cameras, Proceedings of the SPIE 26th International Congress on High-Speed Photography and Photonics, Alexandria, VA, Sept 19, 2004.

8. Gilat, Schmidt and Tyson, Full-Field Strain Measurement During a Tensile Split Hopkinson Bar Experiment, Presented at the SEM Annual Conference and Exposition, St. Louis, June 6, 2006.

9. Schmidt, Gilat, Tyson and Walker, Further Development and Validation of Full-Field Strain Measurements for Hopkinson Bar Testing, Presented at the SEM Annual Conference and Exposition, Springfield, MA, June 5, 2007.

10. Staab, G.H. and Gilat, A., "A Direct-tension Split Hopkinson Bar for High Strain Rate Testing," Exp. Mech., **31 (3)**, 232-235 (1991).